

DNA Ligase IV Suppresses Medulloblastoma Formation¹

Youngsoo Lee and Peter J. McKinnon²

Department of Genetics, St. Jude Children's Research Hospital, Memphis, Tennessee 38105

Abstract

Substantial neural defects are often present in mice with targeted inactivation of DNA repair factors such as DNA ligase IV (Lig4). Whereas *Lig4*^{-/-} mice undergo widespread neural apoptosis and die during development, p53 deficiency rescues this death. We found that all *Lig4*^{-/-}*p53*^{-/-} mice developed medulloblastoma, but did not develop other tumors of the nervous system. *Lig4*^{-/-}*p53*^{-/-} medulloblastoma occurred as early as 21 days of age, originated in the external granule layer of the developing cerebellum, and was synaptophysin immunoreactive. These data reveal a pronounced susceptibility of the cerebellum to the effects of chronic DNA damage and provide a direct link between genotoxic stress and medulloblastoma formation.

Introduction

Maintenance of genomic integrity is of paramount importance for the survival of an organism. Damage to the genome can occur during cellular proliferation (*e.g.*, during S phase), through oxidative damage as a byproduct of cellular metabolism, and also physiologically during meiosis or V(D)J recombination. In these situations, DNA DSBs³ initiate a coordinated cellular response leading to DNA repair and resolution of the break or, alternatively, apoptosis, often via p53-dependent processes. DSBs activate two major repair pathways, NHEJ and HRR, that restore integrity of DNA after endogenous DSBs or those arising from an external agent such as ionizing radiation (1). Compared with HRR, NHEJ repairs DNA breaks without the need for homology between the segments to be rejoined. However, both pathways fulfill indispensable roles and are required for the development and maintenance of higher organisms (1, 2).

Lig4 is a distinct nuclear ligase that is a critical component of NHEJ and is required for V(D)J recombination and DNA repair (3). In addition to Lig4, a number of other proteins are required for NHEJ, including XRCC4, Ku70, Ku80, and the catalytic subunit of DNA-dependent protein kinase (DNA-PK_{CS}/Prkdc). Recent data from mice with inactivation of NHEJ components have shown the absolute requirement of some of the NHEJ components for nervous system development, in addition to their expected roles in immune system function and radiosensitivity (4–10). The additional ablation of *p53* rescues the lethality resulting from *Xrcc4* or *Lig4* deficiency and also leads to the rapid formation of lymphoma in all cases of NHEJ inactivation, underscoring the link between defective DNA repair and tumorigenesis (5, 10–16). In this report, we show that in addition to a high frequency of lymphoma, all *Lig4*^{-/-}*p53*^{-/-} mice develop

medulloblastoma, an embryonal tumor of the cerebellum that occurs with a high incidence in children (17).

Materials and Methods

Animals. *Lig4*^{-/-}*p53*^{-/-} mice were obtained by intercrossing of *Lig4*^{+/-}*p53*^{+/-} or *Lig4*^{+/-}*p53*^{-/-} animals. Lig4 mutant animals used in this study have been described previously (8, 18). All animals were housed in an American Association of Laboratory Animal Care-accredited facility and were maintained in accordance with the NIH Guide for the Care and Use of Laboratory Animals. The institutional animal care and use committee at St. Jude Children's Research Hospital approved all procedures for animal use.

Histology and Immunohistochemistry. Tissue samples from animals of various ages were collected after transcardial perfusion with 4% paraformaldehyde. Fixed tissues were cryoprotected in 25% buffered sucrose solution and cryosectioned (10 μm), or brain tissues were fixed in 10% buffered formalin, embedded in paraffin, and sectioned (5 μm). These sections were stained with H&E according to standard procedures. Immunohistological analyses of tissue were performed using the following antibodies: anti-GFAP (1:400; Sigma); anti-neurofilament 200 (1:500; Sigma); anti-synaptophysin (1:200; Chemicon); anti-MAP2 (1:200; Sigma); anti-β-tubulin III (Tuj1; 1:500; Babco); anti-active caspase 3 (CM1; 0.66 mg/ml; IDUN); and rat anti-CD45R/B220 (1:25; BD PharMingen). Antigen retrieval was used for all antibodies except CD45R/B220. Sections were incubated with antibodies overnight after quenching endogenous peroxidase using 0.6% hydrogen peroxide, and immunoreactivity was visualized with the VIP substrate kit (Vector Laboratories) according to the manufacturer's directions after the tissues were treated with biotinylated secondary antibody and avidin DH-biotinylated horseradish peroxidase-H complex (Vectastain Elite Kit; Vector Laboratories). Sections were counterstained with 0.1% methyl green, dehydrated, and mounted in Permount. For fluorescence signals, FITC, indocarbocyanine (Cy3) or aminomethylcoumarin was used. Apoptosis was measured using Apoptag (Intergen).

Real-time PCR. Total RNA from each tissue sample was extracted using Trizol (Invitrogen) according to the manufacturer's instructions. Real-time PCR was performed using a 7900HT Sequence Detection System (ABI) and the TaqMan One Step PCR Reagent (ABI). RT-PCR was done with following oligonucleotide primer/TaqMan probe sets: (a) Math1 forward (ATGCACGGGCTGAACCA), Math1 reverse (TCGTTGTTGAAGACGGGATA), and Math1 TaqMan probe (CTTCGACCAGCTGCGCAACG); (b) Gli1 forward (GCTTGGATGAAGGACCTTGTG), Gli1 reverse (GCTGATCCAGCCTAAGTCTC), and Gli1 TaqMan probe (CCGACTCTCCAGCCTCCGCC); (c) Gli3 forward (CCCTGCATTGAGCTTCACCTA), Gli3 reverse (AATGCGGAGCCTAAGCTTTG), and Gli3 TaqMan probe (TCTTCACATGCATCAACAGATCCTAAGCCG). The PCR reactions were analyzed using SDS v2.0 software (ABI). Total RNA from the cerebral cortex of neonatal wild-type animals was used to generate standard curves for relative quantitation. 18S rRNA was used as an endogenous control.

Results and Discussion

We rescued the embryonic lethality associated with Lig4 deficiency (8, 18) by additional inactivation of p53 to generate *Lig4*^{-/-}*p53*^{-/-} mice. Previous work has shown that *Lig4*^{-/-}*p53*^{-/-} animals develop pro B-cell lymphoma at a high frequency (11). However, this earlier study did not address the consequence of chronic genotoxic stress toward nervous system function. Analysis of the *Lig4*^{-/-}*p53*^{-/-} brain revealed that at 9 weeks of age, all animals (*n* = 23) had developed medulloblastoma (Fig. 1). As will be detailed below, these medulloblastomas arose independently of pro-B-cell lymphoma.

Received 8/5/02; accepted 10/4/02.

The costs of publication of this article were defrayed in part by the payment of page charges. This article must therefore be hereby marked *advertisement* in accordance with 18 U.S.C. Section 1734 solely to indicate this fact.

¹ Supported by the NIH Grants NS-37956, NS-39867, and CA-21765 and by the American Lebanese and Syrian Associated Charities of St. Jude Children's Research Hospital.

² To whom requests for reprints should be addressed, at Department of Genetics, St. Jude Children's Research Hospital, 332 North Lauderdale Street, Memphis, TN 38105. Phone: (901) 495-2700; Fax: (901) 526-2907; E-mail: peter.mckinnon@stjude.org.

³ The abbreviations used are: DSB, double-strand breaks; Lig4, ligase IV; NHEJ, nonhomologous end joining; HRR, homologous recombination repair.

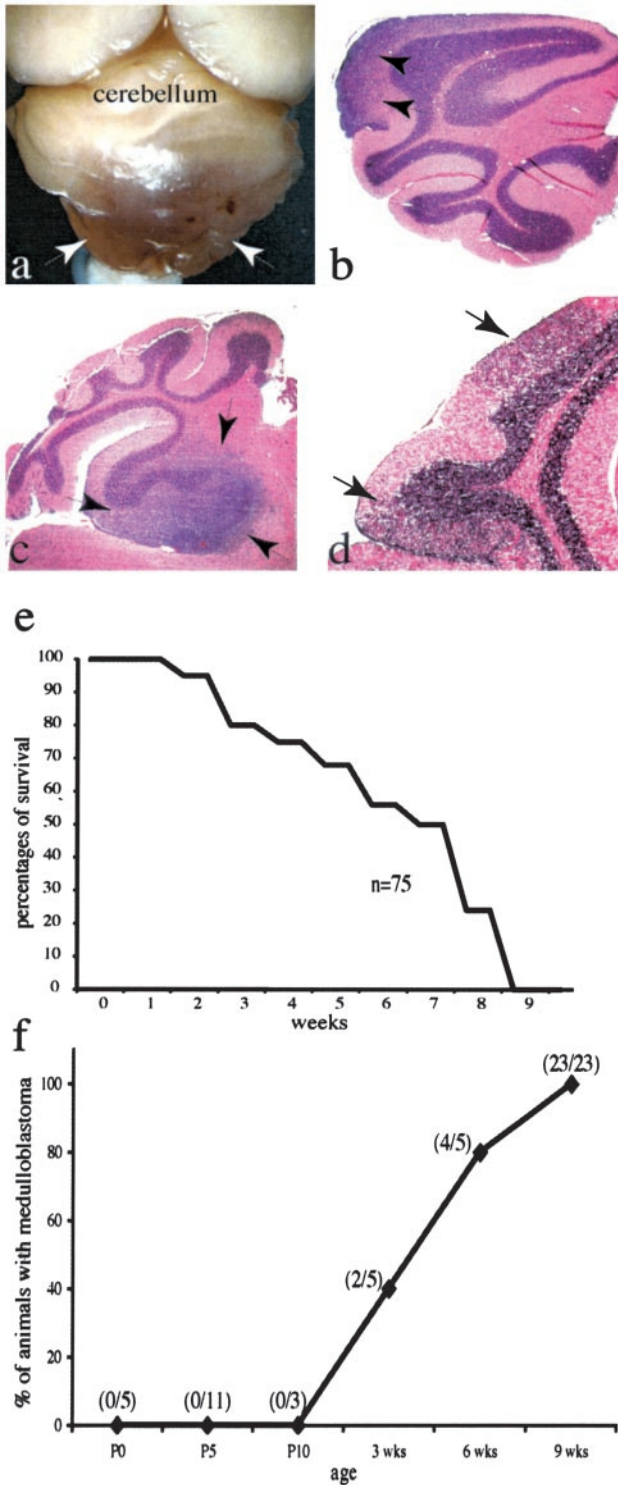


Fig. 1. Lig4 deficiency leads to medulloblastoma. Medulloblastoma in $Lig4^{-/-}p53^{-/-}$ mice occurs at various sites within the molecular layer of the cerebellum. Medulloblastomas from four separate 9-week-old animals are shown in *a-d* (indicated by arrows) and were detectable upon brain isolation (*a*) or when visualized with H&E staining (*b* and *c*). In some cases, multifocal tumor formation is apparent (*d*). None of $Lig4^{-/-}p53^{-/-}$ animals lived longer than 10 weeks of age (*e*). All $Lig4^{-/-}p53^{-/-}$ animals developed medulloblastoma by 9 weeks of age (*f*). Magnification is $\times 4$ for *a*, $\times 40$ for *b* and *c*, and $\times 200$ for *d*.

Whereas these tumors were found in the molecular layer of the cerebellum, the actual site of origin varied within this layer (Fig. 1, *a-d*). In some younger animals, multiple medulloblastomas occurred in widely distant regions of the molecular layer, indicating multiclonal

tumors (Fig. 1*d*). The $Lig4^{-/-}p53^{-/-}$ animals did not survive past 9 weeks of age ($n = 75$) and succumbed to tumor burden from lymphoma, medulloblastoma, or both (Fig. 1*e*). To determine latency of the medulloblastoma, we examined animals at younger ages. Although the incidence of medulloblastoma increased with age until 9 weeks, approximately 50% of $Lig4^{-/-}p53^{-/-}$ mice showed initiating foci of medulloblastoma as early as 3 weeks of age, and most mice had sizable medulloblastoma by 6 weeks of age (Fig. 1*f*).

The $Lig4^{-/-}p53^{-/-}$ medulloblastomas have the typical histology and characteristics of human medulloblastoma (Fig. 2). Tumor foci within the cerebellar external granule layer were found as early as 3 weeks of age and originated at the margin of the external granule layer (Fig. 2, *a* and *b*), consistent with a granule cell origin of this tumor (19). All $Lig4^{-/-}p53^{-/-}$ medulloblastomas examined ($n = 9$) were immunopositive for neural markers including synaptophysin, MAP2, Tuj1, and GFAP (Fig. 2, *d, e*, and *g-i*). However, mature neuronal markers such as neurofilament (NF200), which is strongly expressed in differentiated Purkinje and granule cells (Fig. 2*f*, dashed line and arrow), were absent in the tumor (Fig. 2*f*, asterisk). Even though the medulloblastoma showed positive immunoreactivity for a variety of neuronal markers, we considered the possibility that lymphoma metastasis may contribute to the medulloblastoma because pro-B-cell lymphoma is a characteristic of $Lig4^{-/-}p53^{-/-}$ mice (11). However, immunohistochemistry using lymphocyte markers such as B220 and CD45 was negative for the medulloblastoma (Fig. 2*c*) yet strongly positive for the $Lig4^{-/-}p53^{-/-}$ lymphoma (Fig. 2*c'*). In one case of a 9-week-old $Lig4^{-/-}p53^{-/-}$ mouse that developed both medulloblastoma and lymphoma, we identified infiltrating lymphoma cells that stained strongly for B220 around the meningeal surface of the brain, including a margin around the medulloblastoma (data not shown). However, although we detected strong B220 immunoreactivity in this particular situation, no B220-positive cells were found within the medulloblastoma, nor was this infiltrating lymphoma positive for neuronal markers. The $Lig4^{-/-}p53^{-/-}$ medulloblastomas were also negative for MAC-1 immunoreactivity (a marker for macrophages), and, conversely, the lymphomas were negative for neuronal markers such as MAP2 and Tuj1 (data not shown). Finally, whereas medulloblastomas are present as early as 3 weeks of age before lymphoma onset, a number of older animals were identified that had no discernible lymphoma but had developed medulloblastoma. The $Lig4^{-/-}p53^{-/-}$ medulloblastomas also show high proliferative and apoptotic indices typical of human medulloblastoma (17) as determined by Ki67 and terminal deoxynucleotidyl transferase-mediated nick end labeling staining, respectively (Fig. 2, *j* and *k*). Higher magnification of the medulloblastoma also shows the small round blue cells characteristic of medulloblastoma (Fig. 2*l*).

We did not observe medulloblastoma (or lymphoma) in $Lig4^{-/-}p53^{+/-}$ mice (which are also viable), indicating that complete loss of p53 function is required for early tumor formation. Whereas the $Lig4^{-/-}p53^{-/-}$ medulloblastomas recapitulate many features of the human tumors, p53 mutations have not been considered as a prominent feature of medulloblastoma. However, recent data show that alterations in p53 or the p53 pathway are relatively common in medulloblastoma (20, 21). Lig4 mutations have not been reported in medulloblastoma, although it is likely not many investigators have focused their studies on this gene. Interestingly, mutations in Lig4 are associated with immune dysfunction and developmental abnormalities in a human radiosensitivity syndrome (22), and mutations in Lig4 have been reported in human leukemia (23). However, it is probable that events associated with a lack of DNA repair rather than Lig4 deficiency *per se* result in genomic instability that subsequently leads to medulloblastoma.

The granule cell is the probable cell of origin for medulloblastoma,

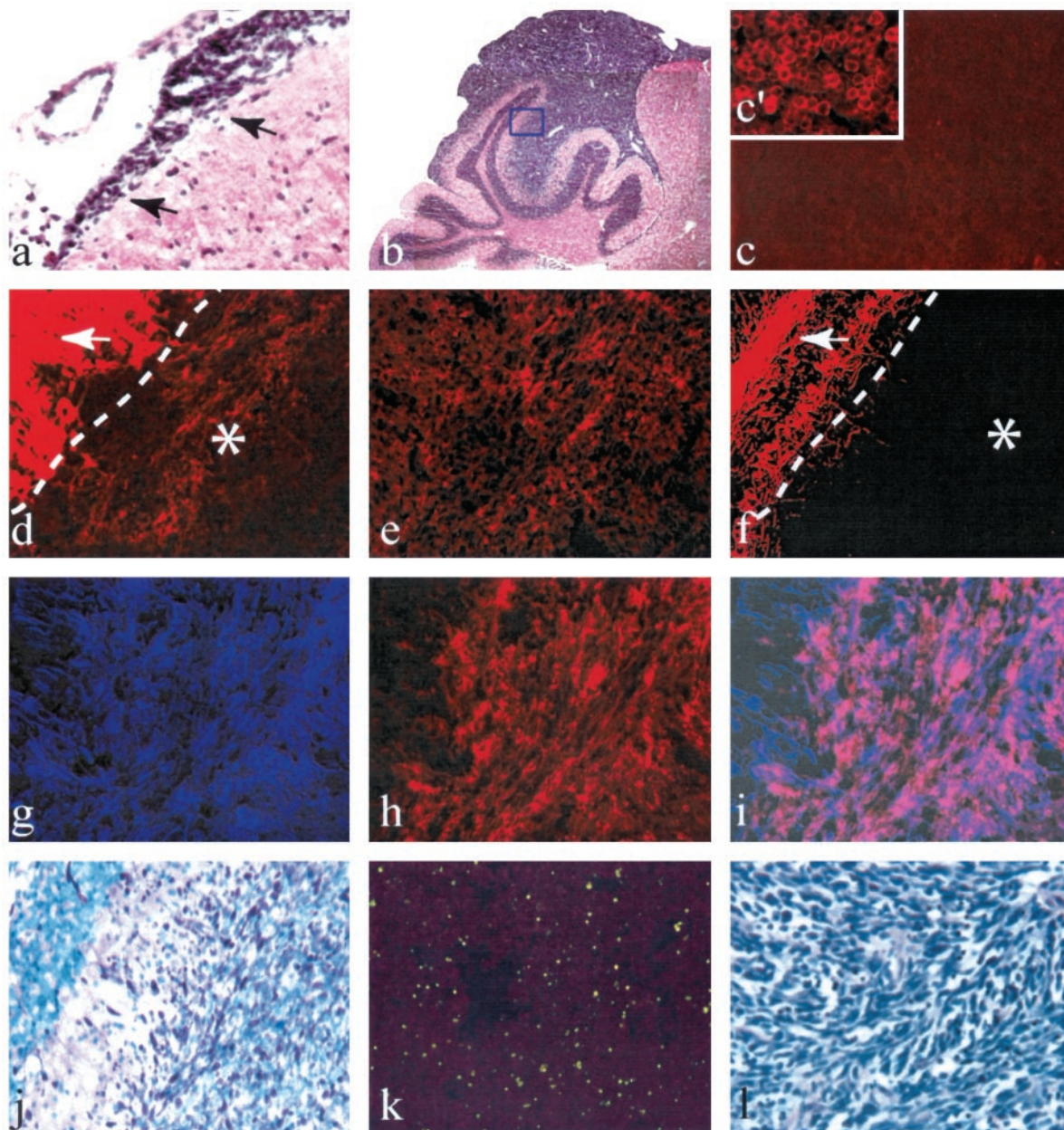


Fig. 2. $Lig4^{-/-}p53^{-/-}$ medulloblastoma characteristics. $Lig4^{-/-}p53^{-/-}$ mice develop medulloblastoma that can be detected as early as 3 weeks of age (a, arrows) and can be sizable at 9 weeks of age (b). Although $Lig4^{-/-}p53^{-/-}$ mice are also prone to develop pro-B-cell lymphoma, medulloblastoma is not immunoreactive for lymphoma markers such as B220 (c), whereas lymphoma is strongly immunoreactive (c'). Medulloblastoma is immunoreactive for synaptophysin (d) and MAP2 (e), but not for mature neuronal markers such as NF200 (f). d and f represent an equivalent region to c-i but have been selected to show the internal granule layer with arrows, the Purkinje layer with a dashed line, and the medulloblastoma with an asterisk. The $Lig4^{-/-}p53^{-/-}$ medulloblastoma also harbors cells that are immunoreactive for both glial (GFAP) and Tuj1 as indicated (g and h), although heterogeneity of expression exists within the tumor as demonstrated when images from g and h are merged (i). The $Lig4^{-/-}p53^{-/-}$ medulloblastoma also shows a high proliferative and apoptotic index as indicated by Ki67 immunoreactivity (j) and terminal deoxynucleotidyl transferase-mediated nick end labeling staining (k). l shows the typical small round blue cells present in the $Lig4^{-/-}p53^{-/-}$ medulloblastoma. a, b, and l are H&E stained. c-j are equivalent magnified views from the boxed area in b. Magnification is $\times 200$ for a, $\times 400$ for b, $\times 400$ for d-k, and $\times 600$ for l.

and therefore we examined the expression of a known germinal granule cell marker *Math1* (the mouse homologue of *Drosophila* Atonal1). In *Math1*-null embryos, the external germinal layer of the cerebellum is missing, implying that *Math1* expression is required to support granule cell genesis (24). Analysis of a number of $Lig4^{-/-}p53^{-/-}$ medulloblastomas showed a high level of *Math1* expression compared with either wild-type age-matched control or developing postnatal day 5 (P5) cerebellum as determined using real-time PCR (Fig. 3a). Furthermore, because the sonic hedgehog pathway is perturbed in some human medulloblastomas (19), we also examined *Gli1*, an important sonic hedgehog target gene. A high

level of *Gli1* expression (but not *Gli3*) was seen in a number of $Lig4^{-/-}p53^{-/-}$ medulloblastomas compared with wild-type controls (Fig. 3, b and c). Notably, for both *Math1* and *Gli1*, there was a striking difference between the expression profile of medulloblastomas and lymphomas isolated from the same animal, further underscoring the distinct origin of each tumor type.

Because only medulloblastoma is found in the $Lig4^{-/-}p53^{-/-}$ nervous system and not other neural tumor types, the cerebellum is particularly sensitive to the effects of genotoxic stress arising from *Lig4* deficiency. The cerebellar granule cell population is the most abundant neuronal population in the nervous system (25); perhaps this

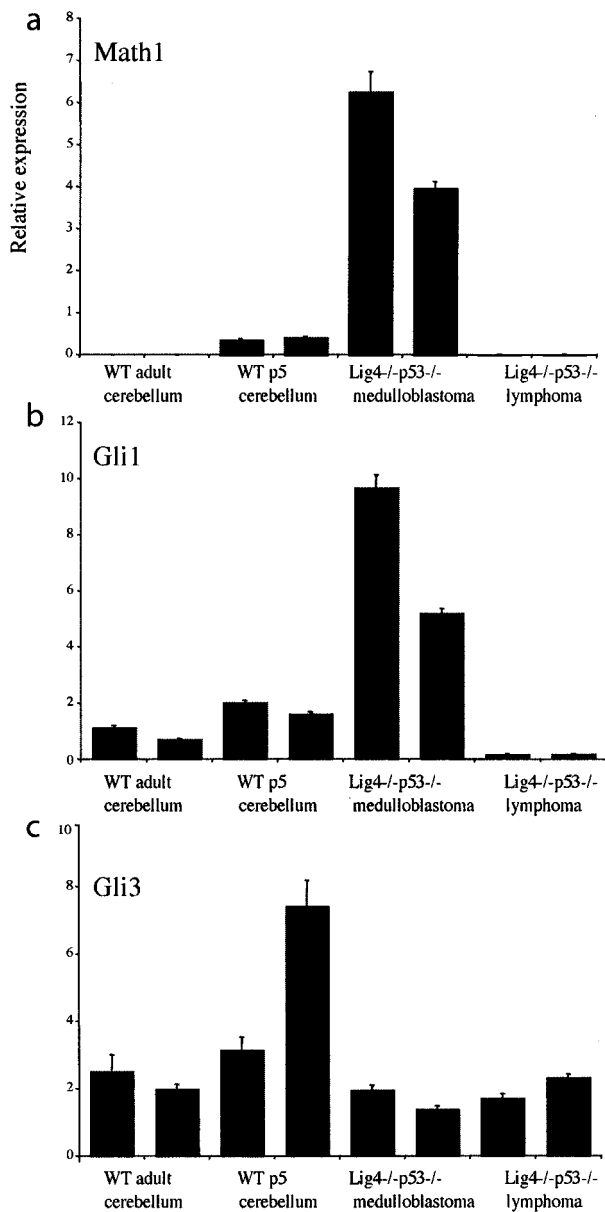


Fig. 3. Gene expression analysis in the *Lig4*^{-/-}*p53*^{-/-} medulloblastoma. Real-time PCR was used to determine the relative expression levels of transcript from the 9-week-old *Lig4*^{-/-}*p53*^{-/-} medulloblastoma compared with wild-type age-matched cerebellum, postnatal day 5 (P5) developing cerebellum, or lymphoma present in the same *Lig4*^{-/-}*p53*^{-/-} animal harboring the medulloblastoma. 18S rRNA was used as an internal standard, and neonatal brain RNA was used as a PCR control for relative expression. Relative expression scales are arbitrary and reflect relative expression within the particular group [Math1 (a), Gli1 (b), or Gli3 (c)].

large target population makes the cerebellum more likely to manifest lesions arising from DNA damage. Supporting this assertion, during early development only a proportion of postmitotic neural cells in the subventricular zone from *Lig4*^{-/-} or *Xrcc4*^{-/-} embryos undergo apoptosis, suggesting that the lesions are stochastic in nature. It will now be of interest to determine whether medulloblastoma occurs in other mouse models where NHEJ or HRR components have been inactivated; the similar neural phenotype of the *Xrcc4*^{-/-} and *Xrcc2*^{-/-} mice (9, 26) to *Lig4* deficiency suggests that this will probably be the case on a p53-null background. Furthermore, because Ku80 functions in the nervous system (6), and *Ku80*^{-/-}*p53*^{-/-} mice develop pro-B-cell lymphoma (14, 15), medulloblastoma may also be a feature of these mice.

Ptc1^{+/-} mutant mice, in a manner similar to humans with *Ptc1* haploinsufficiency, are strongly predisposed to medulloblastoma (19). Notably, *Ptc1* haploinsufficiency leads to radiosensitivity in *Ptc1*^{+/-} mice (27, 28). This radiosensitivity may be due to disruption of appropriate interaction of Ptc1 with phosphorylated cyclin B1 that is required for a DNA damage-induced G₂-M checkpoint (29). Thus, the high incidence of medulloblastoma in the *Lig4*^{-/-}*p53*^{-/-} mice and the relationship between *Ptc1* haploinsufficiency and radiosensitivity suggest that inappropriate responses to genotoxic stress may contribute to some human medulloblastoma.

Acknowledgments

We thank Tomas Lindahl and Deborah Barnes for reagents and advice and Tom Curran and Suzanne Baker for comments on the manuscript.

References

- van Gent, D. C., Hoeijmakers, J. H., and Kanaar, R. Chromosomal stability and the DNA double-stranded break connection. *Nat. Rev. Genet.*, 2: 196–206, 2001.
- Friedberg, E. C., and Meira, L. B. Database of mouse strains carrying targeted mutations in genes affecting cellular responses to DNA damage. Version 4. *Mutat. Res.*, 459: 243–274, 2000.
- Robins, P., and Lindahl, T. DNA ligase IV from HeLa cell nuclei. *J. Biol. Chem.*, 271: 24257–24261, 1996.
- Lee, Y., Barnes, D. E., Lindahl, T., and McKinnon, P. J. Defective neurogenesis resulting from DNA ligase IV deficiency requires *Atm*. *Genes Dev.*, 14: 2576–2580, 2000.
- Gao, Y., Ferguson, D. O., Xie, W., Manis, J. P., Sekiguchi, J., Frank, K. M., Chaudhuri, J., Horner, J., DePinho, R. A., and Alt, F. W. Interplay of p53 and DNA-repair protein XRCC4 in tumorigenesis, genomic stability and development. *Nature (Lond.)*, 404: 897–900, 2000.
- Gu, Y., Sekiguchi, J., Gao, Y., Dikkes, P., Frank, K., Ferguson, D., Hasty, P., Chun, J., and Alt, F. W. Defective embryonic neurogenesis in Ku-deficient but not DNA-dependent protein kinase catalytic subunit-deficient mice. *Proc. Natl. Acad. Sci. USA*, 97: 2668–2673, 2000.
- Gao, Y., Chaudhuri, J., Zhu, C., Davidson, L., Weaver, D. T., and Alt, F. W. A targeted DNA-PKcs-null mutation reveals DNA-PK-independent functions for KU in V(D)J recombination. *Immunity*, 9: 367–376, 1998.
- Barnes, D. E., Stamp, G., Rosewell, I., Denzel, A., and Lindahl, T. Targeted disruption of the gene encoding DNA ligase IV leads to lethality in embryonic mice. *Curr. Biol.*, 8: 1395–1398, 1998.
- Gao, Y., Sun, Y., Frank, K. M., Dikkes, P., Fujiwara, Y., Seidl, K. J., Sekiguchi, J. M., Rathbun, G. A., Swat, W., Wang, J., Bronson, R. T., Malynn, B. A., Brynans, M., Zhu, C., Chaudhuri, J., Davidson, L., Ferrini, R., Stamato, T., Orkin, S. H., Greenberg, M. E., and Alt, F. W. A critical role for DNA end-joining proteins in both lymphogenesis and neurogenesis. *Cell*, 95: 891–902, 1998.
- Ferguson, D. O., and Alt, F. W. DNA double strand break repair and chromosomal translocation: lessons from animal models. *Oncogene*, 20: 5572–5579, 2001.
- Frank, K. M., Sharpless, N. E., Gao, Y., Sekiguchi, J. M., Ferguson, D. O., Zhu, C., Manis, J. P., Horner, J., DePinho, R. A., and Alt, F. W. DNA ligase IV deficiency in mice leads to defective neurogenesis and embryonic lethality via the p53 pathway. *Mol. Cell*, 5: 993–1002, 2000.
- Guidos, C. J., Williams, C. J., Grandal, I., Knowles, G., Huang, M. T., and Danska, J. S. V(D)J recombination activates a p53-dependent DNA damage checkpoint in scid lymphocyte precursors. *Genes Dev.*, 10: 2038–2054, 1996.
- Nacht, M., Strasser, A., Chan, Y. R., Harris, A. W., Schliessel, M., Bronson, R. T., and Jacks, T. Mutations in the p53 and SCID genes cooperate in tumorigenesis. *Genes Dev.*, 10: 2055–2066, 1996.
- Difilippantonio, M. J., Zhu, J., Chen, H. T., Meffre, E., Nussenzweig, M. C., Max, E. E., Ried, T., and Nussenzweig, A. DNA repair protein Ku80 suppresses chromosomal aberrations and malignant transformation. *Nature (Lond.)*, 404: 510–514, 2000.
- Lim, D. S., Vogel, H., Willerford, D. M., Sands, A. T., Platt, K. A., and Hasty, P. Analysis of ku80-mutant mice and cells with deficient levels of p53. *Mol. Cell. Biol.*, 20: 3772–3780, 2000.
- Sharpless, N. E., Ferguson, D. O., O'Hagan, R. C., Castrillon, D. H., Lee, C., Farazi, P. A., Alson, S., Fleming, J., Morton, C. C., Frank, K., Chin, L., Alt, F. W., and DePinho, R. A. Impaired nonhomologous end-joining provokes soft tissue sarcomas harboring chromosomal translocations, amplifications, and deletions. *Mol. Cell*, 8: 1187–1196, 2001.
- Giangaspero, F., Bigner, S. H., Kleihues, P., Pietsch, T., and Trojanowski, J. Q. Medulloblastoma. In: P. Kleihues and W. K. Cavenee (eds.), *Pathology and Genetics of Tumours of the Nervous System*, pp. 129–137. Lyon, France: IARC Press, 2000.
- Frank, K. M., Sekiguchi, J. M., Seidl, K. J., Swat, W., Rathbun, G. A., Cheng, H. L., Davidson, L., Kangaloo, L., and Alt, F. W. Late embryonic lethality and impaired V(D)J recombination in mice lacking DNA ligase IV. *Nature (Lond.)*, 396: 173–177, 1998.
- Wechsler-Reya, R., and Scott, M. P. The developmental biology of brain tumors. *Annu. Rev. Neurosci.*, 24: 385–428, 2001.
- Giordana, M. T., Duo, D., Gasverde, S., Trevisan, E., Boghi, A., Morra, I., Pradotto, L., Mauro, A., and Chio, A. MDM2 overexpression is associated with short survival in adults with medulloblastoma. *Neuro-oncology*, 4: 115–122, 2002.
- Woodburn, R. T., Azzarelli, B., Montebello, J. F., and Goss, I. E. Intense p53 staining

- is a valuable prognostic indicator for poor prognosis in medulloblastoma/central nervous system primitive neuroectodermal tumors. *J. Neurooncol.*, 52: 57–62, 2001.
22. O'Driscoll, M., Cerosaletti, K. M., Girard, P. M., Dai, Y., Stumm, M., Kysela, B., Hirsch, B., Gennery, A., Palmer, S. E., Seidel, J., Gatti, R. A., Varon, R., Oettinger, M. A., Neitzel, H., Jeggo, P. A., and Concannon, P. DNA ligase IV mutations identified in patients exhibiting developmental delay and immunodeficiency. *Mol. Cell*, 8: 1175–1185, 2001.
 23. Riballo, E., Critchlow, S. E., Teo, S. H., Doherty, A. J., Priestley, A., Broughton, B., Kysela, B., Beamish, H., Plowman, N., Arlett, C. F., Lehmann, A. R., Jackson, S. P., and Jeggo, P. A. Identification of a defect in DNA ligase IV in a radiosensitive leukaemia patient. *Curr. Biol.*, 9: 699–702, 1999.
 24. Ben-Arie, N., Bellen, H. J., Armstrong, D. L., McCall, A. E., Gordadze, P. R., Guo, Q., Matzuk, M. M., and Zoghbi, H. Y. *Math1* is essential for genesis of cerebellar granule neurons. *Nature (Lond.)*, 390: 169–172, 1997.
 25. Goldowitz, D., and Hamre, K. The cells and molecules that make a cerebellum. *Trends Neurosci.*, 21: 375–382, 1998.
 26. Deans, B., Griffin, C. S., Maconochie, M., and Thacker, J. *Xrcc2* is required for genetic stability, embryonic neurogenesis and viability in mice. *EMBO J.*, 19: 6675–6685, 2000.
 27. Hahn, H., Wojnowski, L., Zimmer, A. M., Hall, J., Miller, G., and Zimmer, A. Rhabdomyosarcomas and radiation hypersensitivity in a mouse model of Gorlin syndrome. *Nat. Med.*, 4: 619–622, 1998.
 28. Aszterbaum, M., Epstein, J., Oro, A., Douglas, V., LeBoit, P. E., Scott, M. P., and Epstein, E. H., Jr. Ultraviolet and ionizing radiation enhance the growth of BCCs and trichoblastomas in patched heterozygous knockout mice. *Nat. Med.*, 5: 1285–1291, 1999.
 29. Barnes, E. A., Kong, M., Ollendorff, V., and Donoghue, D. J. *Patched1* interacts with cyclin B1 to regulate cell cycle progression. *EMBO J.*, 20: 2214–2223, 2001.